Progress In Electromagnetics Research, Vol. 121, 1–18, 2011

A NEW TRIPLE BAND CIRCULARLY POLARIZED SQUARE SLOT ANTENNA DESIGN WITH CROOKED T AND F-SHAPE STRIPS FOR WIRELESS APPLICATIONS

S. A. Rezaeieh* **and M. Kartal**

Istanbul Technical University, Maslak, Istanbul, Turkey

Abstract—A new design for circularly polarized square slot antenna (CPSSA) is presented. The circular polarization operation in the proposed single-layer antenna is created through two equal sized crooked T-shape and an F-shape strips located on the patch. Compared to most of the previously reported CPSSA structures, the impedance bandwidth and the axial ratio bandwidth of the antenna are increased and also the size of the antenna becomes smaller. The presented CPSSA design has the compact dimensions of $40 \times 40 \times 0.8\,\text{mm}^3$, total impedance matching bandwidth of 8.04 GHz and exhibiting a 28.03% (4.6–6.1 GHz) 3 dB axial ratio bandwidth. A prototype of the antenna is fabricated and tested, and a great agreement with simulated results is obtained.

1. INTRODUCTION

Due to the increasing usage of wireless communication applications, the performance improvement studies of such systems has found a growing investigation area in recent years. Antennas as one of the most important parts of these systems have gained a great attention. Among the various types of antennas, circularly polarized (CP) antennas are the most desired ones, owing to their inevitable merits like reducing polarization mismatch and multipath fading. To benefit from broadband and low profiles, various shapes and designs of broadband circularly polarized slot antennas have been developed to overcome both the narrow impedance and axial-ratio bandwidths (ARBWs) by applying different techniques on patch and ground

Received 15 August 2011, Accepted 28 September 2011, Scheduled 13 October 2011
* Corresponding author: Sasan Ahdi Rezaeieh (sasan.ahdi.rezaieh@gmail.com).

structures [1–30]. Array structures presented in [1, 4, 7] use the same but duplicated structure in different special or phase positions to obtain circular polarization. Patch, microstrip and slot antennas due to their compatibility with integrated circuit systems are also widely used in CP structures [2, 3, 6, 8, 12, 13]. The antennas proposed in [14, 17] have investigated upon embedding two inverted-L grounded strips around two opposite corners of the slot, each of which using different feedline shapes. Embedding two spiral slots is also presented in [15], in which current circulation in the spiral slots are employed to achieve the CP operation. Utilizing a shorted square-ring slot is another way of creating CP antennas which is presented in [16]. Recently some annular-ring slots [18, 20] are employed to achieve the CP characteristic. In these antennas the circular polarization is attained through a double-bent microstrip line that feeds the antenna at two different positions. In [19], C-like monopole with one sleeve is used in order to excite the CP and improve the impedance bandwidth of the antenna. Asymmetric square slot presented in [21, 22] provides a CP bandwidth which is larger than 10% simply by using an inverted-L tuning stub protruded from the signal line of the coplanar waveguide (CPW). In the stair-shaped slot presented in [23], CP operation is obtained by etching a longitudinal slot at a middle point of a stair-shaped slot. In [24], by introducing the corrugated slot and meander line, both the impedance bandwidth and CP bandwidth could be improved. Finally ring slot antenna, reported in [25], achieves CP radiation by introducing proper asymmetry in the ring slot structure and feeding the ring slot using a microstrip line at 45° from the introduced asymmetry.

All of the discussed antennas have large dimensions which are not appropriate to be used in wireless communication systems. Also most of them have either small ARBWs or narrow impedance matching bandwidth. Starting with this motivation, in this letter, a new triple band, compact CPW-fed, circularly polarized square slot antenna with dual monopole feed and crooked F and T-strips is presented. The antenna has three functional bands operating from 1.96 GHz to 3.26 GHz, 3.61 GHz to 6.98 GHz and 7.87 GHz to 11.24 GHz. This design (for the optimized values) supports the three bandwidths in terms of impedance matching but for the 3 dB ARBW, it supports only the second band. Employing dual monopole structure enhances the antenna with large bandwidth and small size. Also the proposed antennas in this paper has the capability of showing CP characteristics in the important standards such as IEEE 802.11b/g (2.4–2.484 GHz), IEEE 802.11a (5.15–5.35 GHz and an additional band of 5.725–5.825 GHz), and HiperLAN2 (5.47–5.725 GHz) [28, 29].

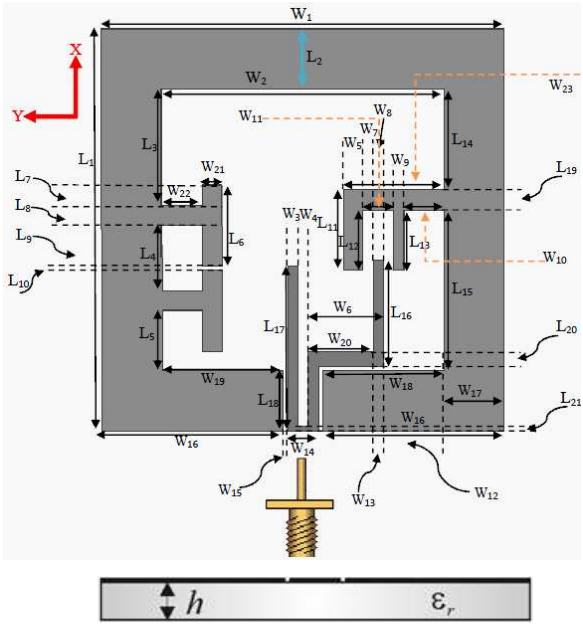

Figure 1. Geometry of the proposed CP triple band antenna ($L_1 = 40$, $L_2 = 6$, $L_3 = 11.5$, $L_4 = 6.5$, $L_5 = 6$, $L_6 = 8$, $L_7 = 2$, $L_8 = 2$, $L_9 = 4$, $L_{10} = 0.5$, $L_{11} = 8$, $L_{12} = 6$, $L_{13} = 6$, $L_{14} = 10$, $L_{15} = 16$, $L_{16} = 10.5$, $L_{17} = 16.5$, $L_{18} = 6$, $L_{19} = 2$, $L_{20} = 2$, $L_{21} = 0.5$ $W_1 = 40$, $W_2 = 28$, $W_3 = 1$, $W_4 = 1$, $W_5 = 2$, $W_6 = 7.5$, $W_7 = 1$, $W_8 = 1$, $W_9 = 1$, $W_{10} = 4$, $W_{11} = 3$, $W_{12} = 6$, $W_{13} = 1$, $W_{14} = 3$, $W_{15} = 0.5$, $W_{16} = 18$, $W_{17} = 6$, $W_{18} = 12$, $W_{19} = 12$, $W_{20} = 6.5$, $W_{21} = 2$, $W_{22} = 4$, $W_{23} = 11$) (Unit: mm).

2. ANTENNA DESIGN AND CONFIGURATION

The proposed circularly polarized square slot (CPSS) antenna geometry and its dimensions are presented in Figure 1. The configuration of the antenna is combination of the dual-monopole antenna [26] and the square slot CP antenna [27]. As a result, the proposed antenna inherits a wide CP bandwidth. The antenna is printed on a FR4 dielectric substrate with a thickness of 0.8 mm, $\varepsilon_r = 4.4$ and loss tangent of $\tan\delta = 0.02$. Total dimension of the antenna is as compact as $40 \times 40 \times 0.8\,\text{mm}^3$. The antenna is fed by a 50 Ω CPW with a signal strip of 3 mm width and two identical gaps of 0.5 mm width. The feed line is terminated with a standard SMA connector. Two main features incorporated into the design are

enhancing the ARBW and enlarging the impedance bandwidth. For achieving efficient excitation and good impedance matching, the signal strip of the CPW should be protruded into the square slot. In general, the length of monopole antenna is usually about a quarter-wavelength. The approximate value for the length L_{16} of monopole radiating strip is then given by $L_{16} = \frac{\lambda_g}{4}$, and λ_g is

$$\lambda_g = \frac{\lambda_r}{\sqrt{\varepsilon_{eff}}} = \frac{c}{\sqrt{\varepsilon_{eff}} f_r} \tag{1}$$

$$\varepsilon_{eff} = \frac{\varepsilon_r + 1}{2} \tag{2}$$

where in (1), c is the speed of light, λ_r is the free-space wavelength of the monopole resonant frequency f_r, and in (2) ε_{eff} is the approximated effective dielectric constant [30]. There are two deformed parallel monopoles in the feeding line. Their lengths are selected as $L_{17} = 0.58L_s$ and $L_{16} = 0.37L_s$ where $L_s = L_3 + 2L_8 + L_4 + L_5$. The width of the monopole on the right side is selected as $W_{20} = 0.16W_2$. Due to the presence of different lengths of the two monopoles, the first resonant frequency of the proposed antenna is expected to be controlled mainly by the length of the longer monopole, and the second resonant frequency is greatly dependent on the length of the shorter monopole. The gap between these two monopoles is adjusted to be 1 mm. Unlike the T-shaped strips used in most of the conventional CPW-fed CP antennas a cactus shaped strip is adopted in the presented design. Dual monopole antenna is used to enhance the antenna with wider bandwidth, since the dual monopole structure creates two resonant frequencies and by carefully adjusting the elements of the dual monopole, antenna can support a wider operating frequency band. To generate an asymmetrical feeding stub and thus excite the new resonance modes for improving the CP and impedance bandwidth, a strip with dimensions of 1 mm × 7.5 mm is cut and removed from the feedline; a further study is done on the effect of this strip on the impedance matching and 3 dB ARBWs of the antenna in Section 3. The simulation results show that embedding the arms (L_{16} and L_{17}) to the feedline and adjusting their lengths increases the impedance matching bandwidth. In the CPSS design, a crooked F-shape strip and two equal sized crooked T-shape strips are embedded as shown in Figure 1. The CP operation of the proposed antenna is mainly attributed to the two grounded crooked-T and a crooked-F metallic strip placed at the center of the square slot to excite two orthogonal radiation fields with equal amplitudes. The combination of the feedline and the crooked F and T-strips, which lead to a large ARBW, may not guarantee a satisfying impedance matching, and tuning the distance

between the crooked F and T-strips on the grounded patch is required. In the antenna structure presented in Figure 1, during several tests and simulations, it could be understood that the circular polarization operation of the antenna is principally interrelated to the grounded F and T strips placed around two bottom corners of the square slot.

3. PARAMETRIC STUDY OF THE ANTENNA

Through Figure 2 four improved designs of the proposed CPSS antenna are presented. The antenna design is started by applying a simple strip feedline (Ant. 0) and then improved through adding arms (L_{16} and L_{17}) to the feedline to form a cactus shape. A further improvement is achieved by etching a tuning slit on the feedline to obtain a wide impedance matching bandwidth (Ant. I). -10 dB impedance matching curves of the antenna are presented in Figure 3. As it is observed from Figure 3, by employing a simple strip as the feedline, a great impedance mismatch is experienced (black curve) and consequently any bandwidth of the antenna under -10 dB is available. By adding arms to the simple strip feedline, antenna operates between 2.9 GHz $\sim$ 3.5 GHz and 4.8 GHz $\sim$ 10.5 GHz (blue curve). The optimized feed line

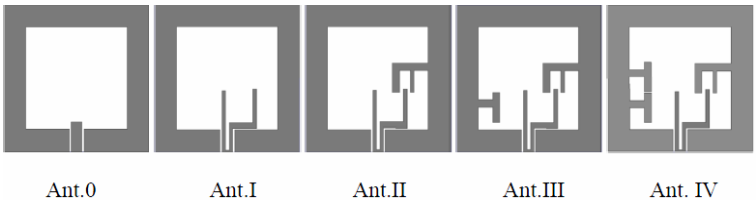

Figure 2. Four improved prototypes of the antenna.

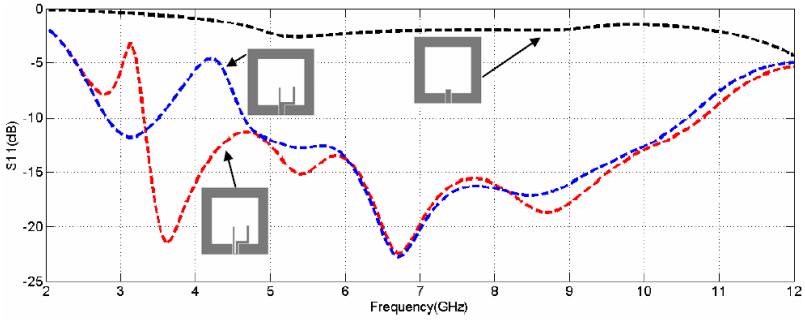

Figure 3. Improved S_{11} of the antenna.

structure (Ant. I) is created through cutting a strip from the feedline (red curve). The simulation results show that embedding the arms to the feedline (Ant. 0–Ant. IV) and adjusting the parameters, an improvement on the impedance bandwidth as well as CP characteristic can be accomplished for the proposed antenna.

As Jou et al. presented in [30], the general behavior of a monopole antenna is either vertical or horizontal linearly polarized. To obtain CP operation by exciting two orthogonal polarizations, the design is improved by adding a crooked F-shape strip to the right bottom corner of the structure. This structure is presented as Ant. II in Figure 2. Return loss variations of Ant. I–Ant. IV are presented

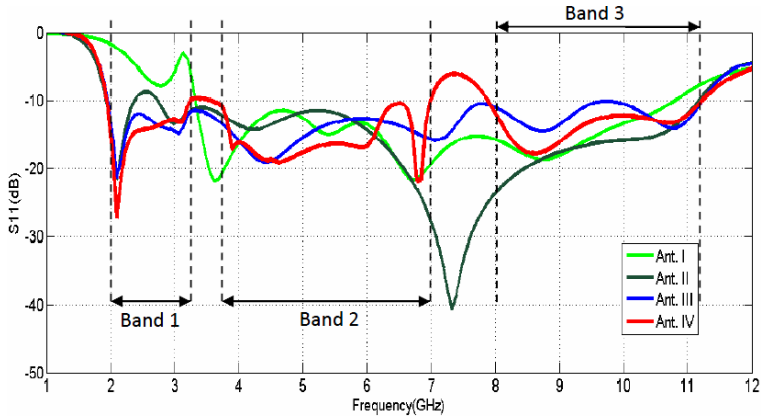

Figure 4. S_{11} of the proposed antennas in Figure 2.

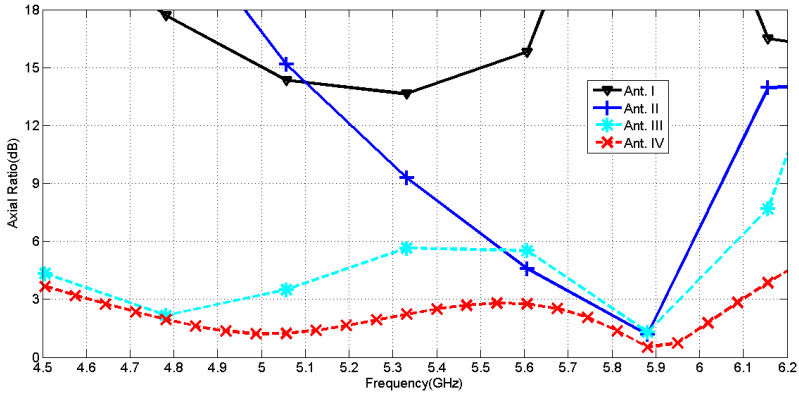

Figure 5. Axial ratio of the proposed antennas in Figure 2.

in Figure 4. Considering the CP characteristic of the antenna, the changing regulation of the right hand side monopole is similar to that of left hand side one. Through Figure 5 it can be observed that by adding a crooked F-shape to the antenna structure, a small improvement in the axial ratio of the antenna is created, and antenna operates CP about 3.2% (5.72 $\sim$ 5.91 GHz). To further improve the CP characteristic of the antenna, two crooked T-shape strips are sequentially added to the structure. As it is seen from Figure 4, adding strips to Ant. I make the antenna operate triple band, and in the final design (Ant. IV), 404 MHz (26.9%) extra bandwidth is obtained compared to the Ant. I. It can be seen in Figure 5 that the ARBW of the antenna increased to 4.7 $\sim$ 4.95 GHz and 5.78 $\sim$ 5.95 GHz for Ant. III and 4.6 $\sim$ 6.1 GHz for the final structure (Ant. IV) respectively. In order to investigate the effects of various parameters on the antenna performance, parametric study has been carried out by

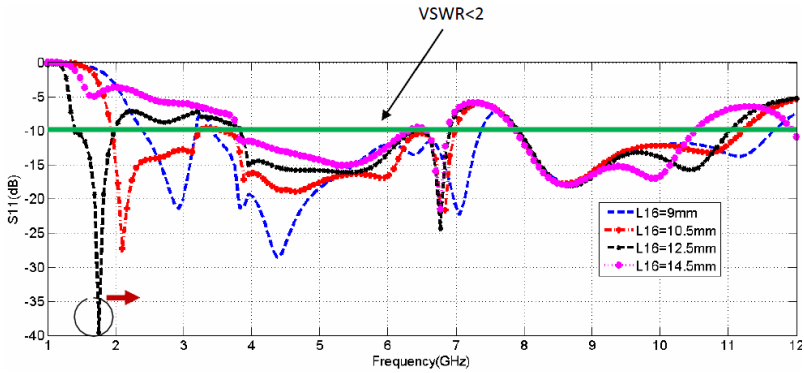

Figure 6. S_{11} for different iterations of L_{16}.

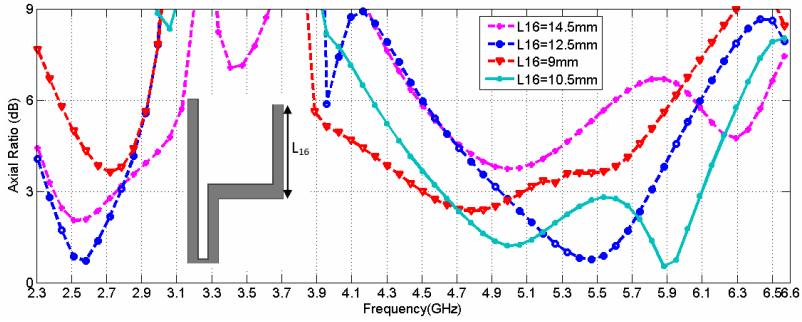

Figure 7. Axial ratio for different iterations of L_{16}.

the Ansoft High Frequency Structure Simulator (HFSS). Except the studied parameters, all the other parameters are fixed to the values as in Figure 1.

3.1. Studying Effects of L_{16}

The simulated 10 dB return loss and axial ratio bandwidths for different lengths of the L_{16} parameter of the dual monopole antenna is presented in Figures 6 and 7 respectively. The optimized value of the L_{16} is given in Section 2. It can be observed that increasing the length of L_{16}, causes a decrease on the center frequencies of all three impedance bands. But the change of the first band is more noticeable. The impedance matching bandwidths of the first and third bands become much smaller when the length of L_{16} increases, while the second band

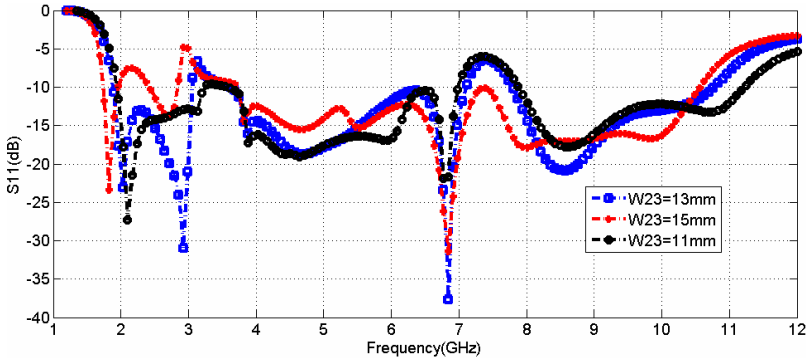

Figure 8. S_{11} for different iterations of W_{23}.

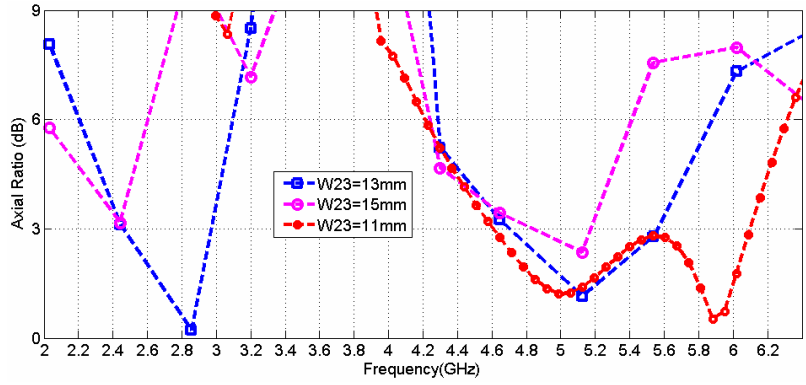

Figure 9. Axial ratio for different iterations of W_{23}.

becomes much wider. On the other hand increasing the length of L_{16}, creates the CP at the first band, between $2.38 \sim 2.78$ GHz, but through Figure 6, it could be understood that the CP bandwidth does not guarantee the impedance matching bandwidth for the same frequency band.

3.2. Studying Effects of W_{23}

Picking $W_{23} = 11$ mm (optimized value), enhances the antenna with maximum axial ratio of 28.03% for the final design (Ant. IV). Even small changes in this parameter (W_{23}) leads to considerable variations in both impedance matching and 3 dB axial ratio bandwidths of the antenna. To highlight these variations, different values of W_{23} are studied. As presented in Figures 8 and 9, by increasing W_{23}, center frequencies of all three operating bands move to lower frequencies and a decrease in impedance matching bandwidth is experienced.

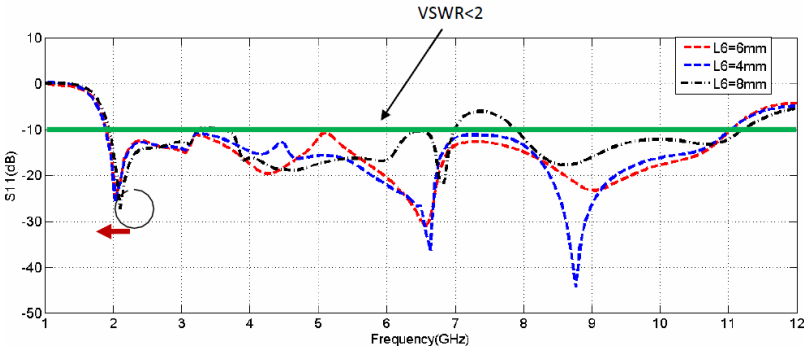

Figure 10. S_{11} for different iterations of L_6.

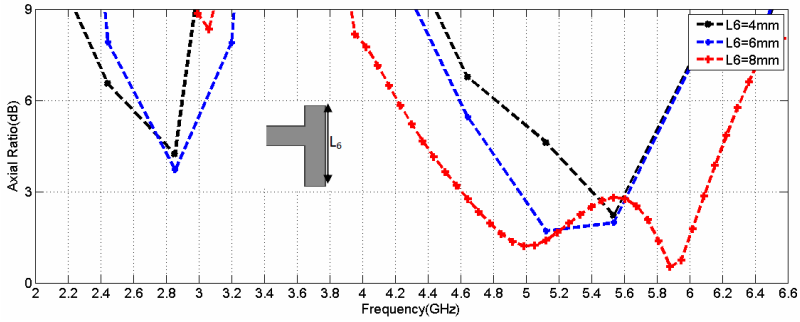

Figure 11. Axial ratio for different iterations of L_6.

Considering the ARBW, for $W_{23} = 13\,\text{mm}$, a new lower band CP characteristic, between 2.4 GHz and 2.9 GHz is created which covers the IEEE 802.11b/g standard for wireless local area network (WLAN), but the second band ARBWs degrades about 600 MHz. Although there is no change in the overall ARBWs of the antenna, the antenna covers all IEEE 802.11a, a band of 5.15–5.35 GHz and HiperLAN2, a band of 5.47–5.725 GHz besides the band of 5.15–5.35 GHz which is very desirable.

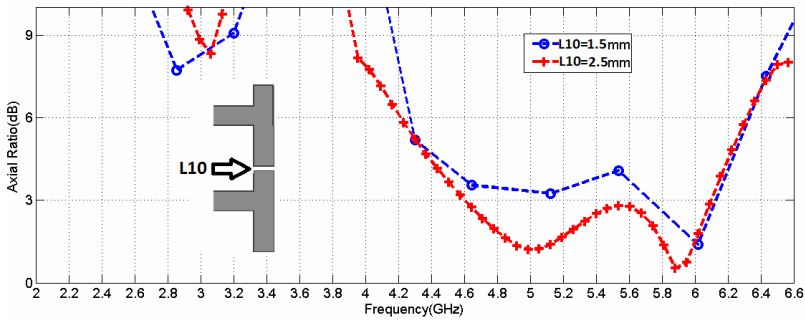

Figure 12. Axial ratio for different iterations of L_{10}.

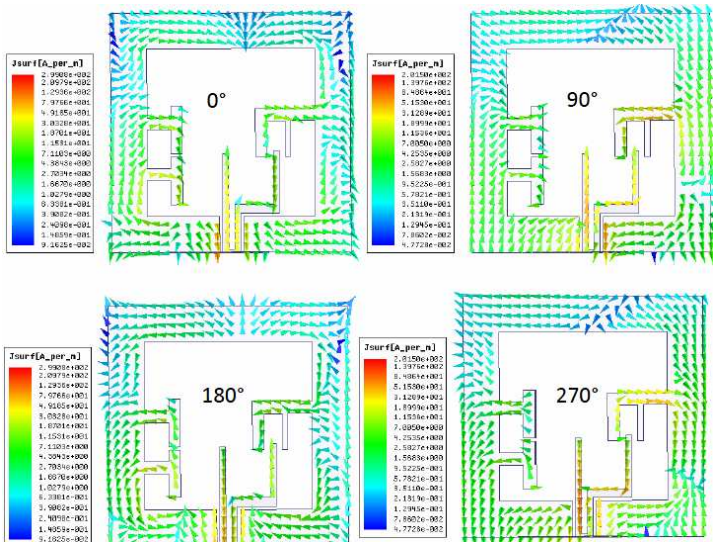

Figure 13. Distribution of the surface current on the feed and ground of the CPSS antenna at 5.4 GHz in 0°, 90°, 180°, and 270° phase.

3.3. Studying Effects of L_6 and L_{10}

Through extensive simulations and experiments, it was found that length of the crooked T-shape strips should be selected as $0.28L_s$, and the distance between them should be $0.23L_s$, to attain the 28.03% ARBW. Changing the length or distance between these strips will degrade the axial ratio and subsequently CP characteristic of the antenna seriously. Considering Figures 10 and 11, it is understood that changing the size of L_6 to $0.21L_s$ and $0.14L_s$, will cause a slight shift to the left in the first resonance frequency of the antenna in the first band and a slight shift to the right in the third band. Adjusting $L_6 = 0.21L_s$, an UWB CPSS antenna will be obtained which its ARBW is 13.33% and covers more than 141% of frequency band. By setting $L_6 = 0.14L_s$, again an UWB antenna is obtained which has the same frequency characteristics as previous one ($L_6 = 0.21L_s$), but ARBW of the antenna degrades as much as 1.3 GHz compared to the optimized antenna. The optimized antenna structure (Ant. IV) is also sensitive to the distance between the crooked T-strips, which is presented by L_{10}. Through extensive simulations and empirical

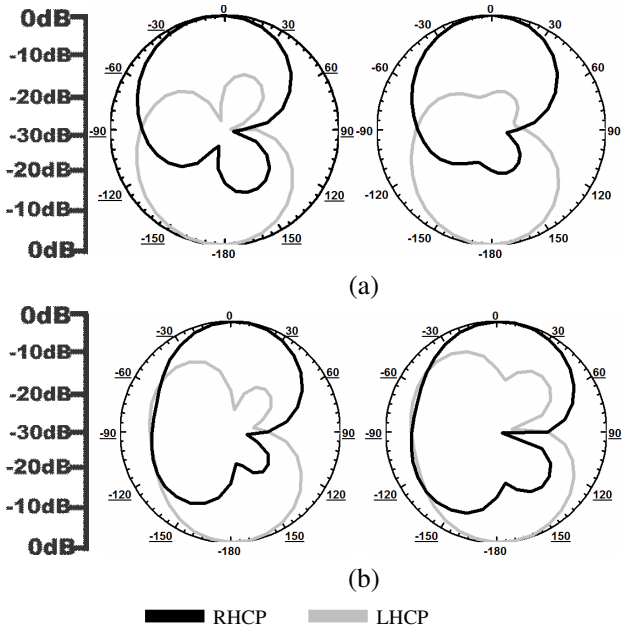

Figure 14. Measured radiation patterns of the antenna at 4.8 GHz (Left) and 5.3 GHz (Right) at (a) $\varphi = 0°$, (b) $\varphi = 90°$.

experiences, the distance between the crooked T-shaped strips was optimized as 0.5 mm. The effect of L_{10} variations on the ARBWs of the antenna is studied and results are presented in Figure 12. Setting $L_{10} = 1.5$ mm will degrade the 3 dB axial ratio bandwidth seriously as 1.1 GHz. Increasing the L_{10} will also cause poverties in the ARBW which are not presented.

To illustrate the circular polarization mechanism, which requires modes of equal magnitude that are in opposite phase, the simulated surface current distributions viewed from the microstrip side are illustrated in Figure 13. The direction of the surface currents on the dipole arms and the microstrip feed network is presented at 5.4 GHz as the phase changes from 0 through 270 degrees. It is observed that the surface current distribution in 90 and 270 degrees are equal in magnitude and opposite in phase as in 0 and 180 degrees. Antenna shows mainly RHCP at $z > 0$ and LHCP at $z < 0$. Measured RHCP and LHCP radiation patterns and directivity of the antenna at typical frequencies of 4.8 GHz and 5.3 GHz are presented at Figure 14. Finally prototypes of the optimized antennas (Ant. I–Ant. IV) are fabricated and measured. Photographs of the antennas are shown in Figure 15. Measured and simulated return loss and 3 dB axial ratio bandwidth of the optimized antenna (Ant. IV) are presented in Figure 16 and

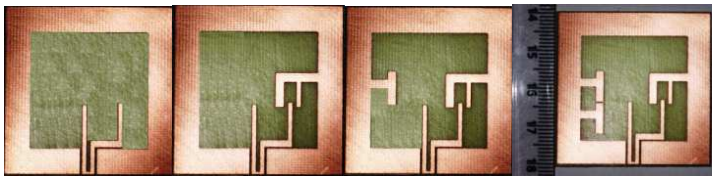

Figure 15. Photograph of the four prototypes of CPSS antennas.

Table 1. Measured S_{11} and 3 dB ARBWs of CPSS antennas.

	BW (VSWR < 2) MHz	**3 dB ARBW (%)**
Ant. I	3423–1091	0
Ant. II	1823–2283 2821–11131	3.76%
Ant. III	1795–9621 9821–10096	2.05%
Ant. IV	1871–3321 3731–7012 7887–11196	28.03%

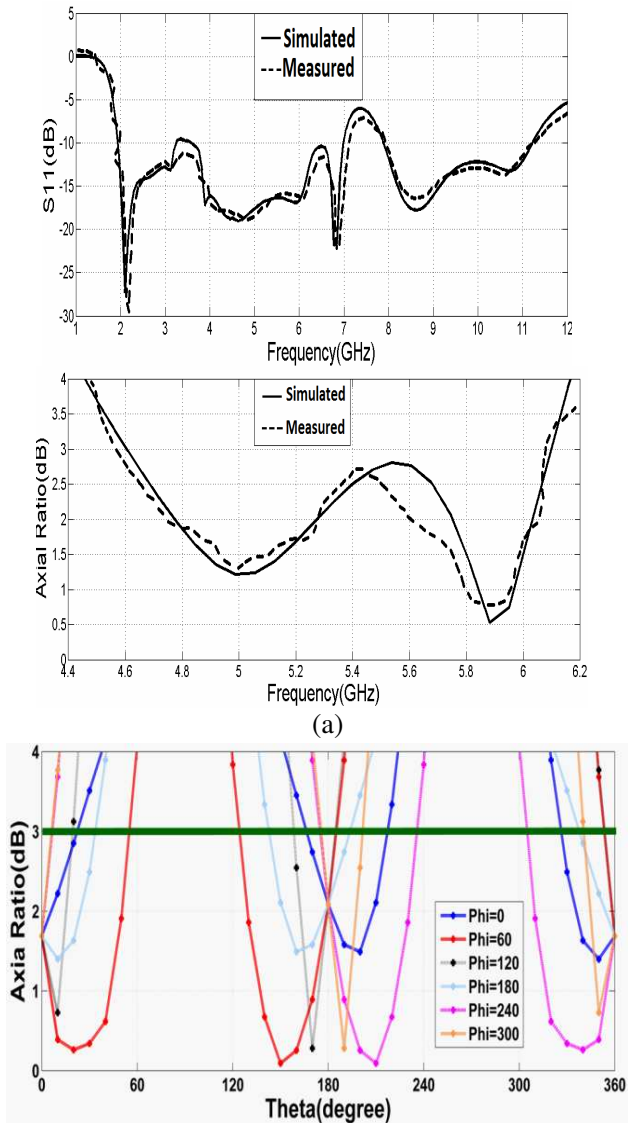

Figure 16. Measured and simulated (a) impedance matching and 3 dB axial ratio bandwidths of the proposed CPSSA with frequency and (b) different φ angles at sample frequency of 5 GHz.

in addition, return loss and 3 dB ARBW of the Ant. I–Ant. IV are presented in Table 1.

A good agreement is observed between the measured and

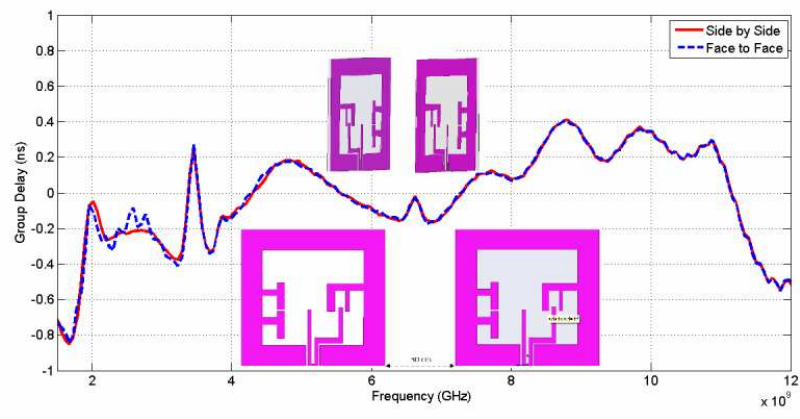

Figure 17. Measured group delay of the antenna.

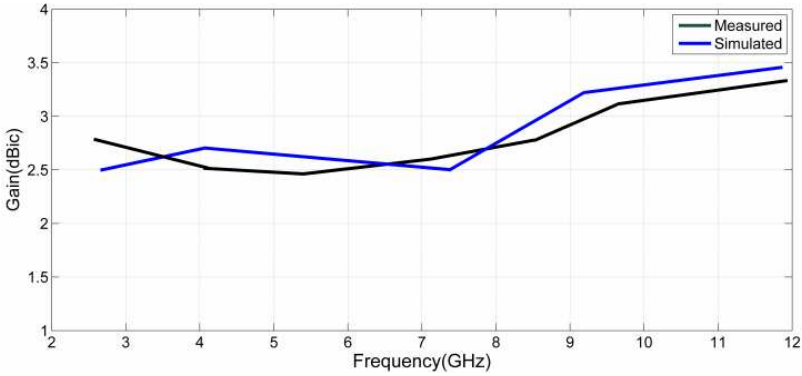

Figure 18. Measured and simulated gain of the CPSSA.

simulated data. One can observe a small difference between measured and simulated data at center frequencies. This might be due to other unknown parasitic effects which are not considered in the simulation. Since the soldering is not done with a machine on the PCB, positional errors might give rise to the discrepancy. The face to face and side to side group delay of the optimized antenna is also measured and presented in Figure 17. As it is obvious, the measured group delay of the antenna is under 0.5 ns which is very desirable for a low delay communication. Measured and simulated gains of the antenna are shown in Figure 18. Antenna can attain a measured peak gain of 3.3 dBi. The current surface of the antenna at sample frequency of 5 GHz is also presented in Figure 19. It can be seen from the plots, the

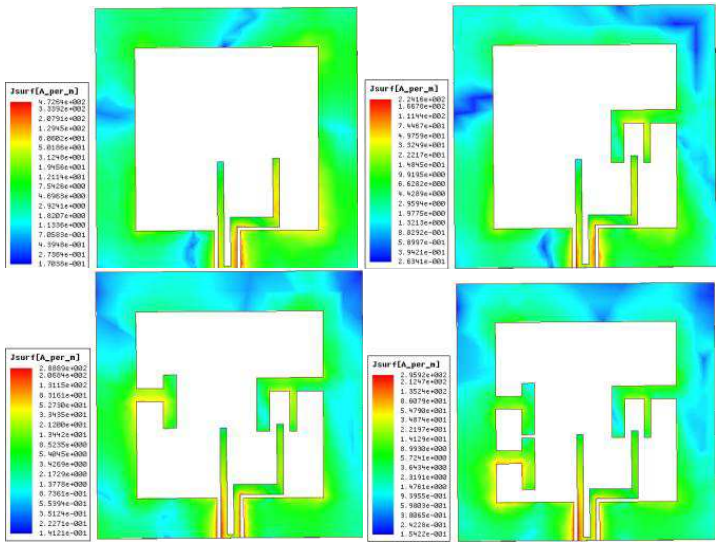

Figure 19. Distribution of the surface current on the feed and ground of the CPSS antenna at 5 GHz.

current concentration of the antenna after adding the strips is at the lower center of the patch.

4. CONCLUSION

A design procedure has been developed for a CP square slot antenna having a 3 dB ARBW. The antenna has a better impedance matching and 3 dB AR bandwidths with a more compact size compared to the most of previously reported wide slot antennas. The normalized antenna areas of the designed antenna is as small as $40 \times 40\,\text{mm}^2$, yet the CP band have a 3 dB ARBW of as large as 28.03% and can be completely enclosed by the corresponding VSWR $\leq$ 2 impedance bands. With a simple dual monopole feedline the resulting antenna became very small and is more suitable for handheld wireless applications.

REFERENCES

1. Liao, W.-J., S.-H. Chang, Y.-C. Chu, and W.-S. Jhong, "A beam scanning phased array for UHF RFID readers with

circularly polarized patches," *Journal of Electromagnetic Waves and Applications*, Vol. 24, Nos. 17–18, 2383–2395, 2010.

2. Hong, T., L.-T. Jiang, Y.-X. Xu, S.-X. Gong, and W. Jiang, "Radiation and scattering analysis of a novel circularly polarized slot antenna," *Journal of Electromagnetic Waves and Applications*, Vol. 24, No. 13, 1709–1720, 2010.
3. Ooi, T. S., S. K. A. Rahim, and B. P. Koh, "2.45 GHz and 5.8 GHz compact dual-band circularly polarized patch antenna," *Journal of Electromagnetic Waves and Applications*, Vol. 24, Nos. 11–12, 1473–1482, 2010.
4. Lin, C., F.-S. Zhang, Y. Zhu, and F. Zhang, "A novel three-FED microstrip antenna for circular polarization application," *Journal of Electromagnetic Waves and Applications*, Vol. 24, Nos. 11–12, 1511–1520, 2010.
5. Du, S., Q.-X. Chu, and W. Liao, "Dual-band circularly polarized stacked square microstrip antenna with small frequency ratio," *Journal of Electromagnetic Waves and Applications*, Vol. 24, Nos. 11–12, 1599–1608, 2010.
6. Chiu, C.-N. and C.-C. Yang, "A new board-integrated single microstripfed circularly polarized monopole antenna for global positioning satellite receivers," *Journal of Electromagnetic Waves and Applications*, Vol. 24, No. 7, 903–909, 2010.
7. Li, X., Y.-J. Yang, X. Tao, L. Yang, S.-X. Gong, Y. Gao, K. Ma, and X.-L. Liu, "A novel design of wideband circular polarization antenna array with high gain characteristic," *Journal of Electromagnetic Waves and Applications*, Vol. 24, No. 7, 951–958, 2010.
8. Deng, S.-M., C.-L. Tsai, M.-F. Chang, and S.-S. Bor, "A study on the non-uniform rectangularring slot antenna for broadband circular polarization operations," *Journal of Electromagnetic Waves and Applications*, Vol. 24, No. 4, 543–555, 2010.
9. Lai, C.-H., T.-Y. Han, and T.-R. Chen, "Circularly-polarized reconfigurable microstrip antenna," *Journal of Electromagnetic Waves and Applications*, Vol. 23, Nos. 2–3, 195–201, 2009.
10. Tsai, C.-L., S.-M. Deng, C.-K. Yeh, and S.-S. Bor, "A novel shorted rectangular-loop antenna for circularly polarized wave operations," *Journal of Electromagnetic Waves and Applications*, Vol. 23, No. 10, 1323–1334, 2009.
11. Bai, X., X. M. Zhang, L. Li, Q. Yang, and J. Y. Li, "Double-sided printed four rhombic-loop antenna with parasitic loops for circular polarization," *Journal of Electromagnetic Waves and Applications*, Vol. 23, No. 13, 1795–1802, 2009.

12. Chen, J., G. Fu, G.-D. Wu, and S.-X. Gong, "Broadband circularly polarized combinatorial slot antenna," *Journal of Electromagnetic Waves and Applications*, Vol. 23, No. 16, 2127–2134, 2009.
13. Wang, A.-N. and W.-X. Zhang, "Design and optimization of broadband circularly polarized wide-slot antenna," *Journal of Electromagnetic Waves and Applications*, Vol. 23, No. 16, 2229–2236, 2009.
14. Pourahmadazar, J., C. Ghobadi, J. Nourinia, N. Felegari, and H. Shirzad, "Broadband CPW-fed circularly polarized square slot antenna with inverted-L strips for UWB applications," *IEEE Antennas and Wireless Propagation Letters*, Vol. 10, 2011.
15. Chen, C. and E. K. N. Yung, "Dual-band dual-sense circularly-polarized CPW-fed slot antenna with two spiral slots loaded," *IEEE Transactions on Antennas and Propagation*, Vol. 57, No. 6, Jun. 2009.
16. Chang, K.-M., R.-J. Lin, I.-C. Deng, and Q.-X. Ke, "A novel design of a microstrip fed shorted square-ring slot antenna for circular polarization," *Microwave and Optical Technology Letters*, Vol. 49, No. 7, Jun. 2007.
17. Sze, J., C. I. G. Hsu, Z. W. Chen, and C. C. Chang, "Broadband CPW-fed circularly polarized square slot antenna with lightening-shaped feedline and inverted-L grounded strips," *IEEE Transactions on Antennas and Propagation*, Vol. 58, No. 3, Mar. 2010.
18. Sze, J., C. I. G. Hsu, M. Ho, Y. Ou, and M. Wu, "Design of circularly polarized annular-ring slot antennas fed by a double-bent microstripline," *IEEE Transactions on Antennas and Propagation*, Vol. 55, No. 11, Nov. 2007.
19. Wang, C.-J. and Y.-C. Lin, "New CPW-fed monopole antennas with both linear and circular polarizations," *IET Microw. Antennas Propag.*, Vol. 2, No. 5, 466–472, 2008.
20. Sze, J. and W. H. Chen, *Axial-ratio-bandwidth Enhancement of a Microstrip-line-fed Circularly Polarized Annular-ring Slot Antenna*, IEEE Early Access, 2011.
21. Sze, J.-Y., J.-C. Wang, and C.-C. Chang, "Axial-ratio bandwidth enhancement of asymmetric-CPW-fed circularly-polarised square slot antenna," *Electronics Letters*, Vol. 44, No. 18, Aug. 28, 2008.
22. Fu, S., S. Fang, Z. Wang, and X. Li, "Broadband circularly polarized slot antenna array fed by asymmetric CPW for L-band applications," *IEEE Antennas and Wireless Propagation Letters*, Vol. 8, 2009.

23. Wang, C.-J. and C.-H. Chen, "CPW-fed stair-shaped slot antennas with circular polarization," *IEEE Transactions on Antennas and Propagation*, Vol. 57, No. 8, Aug. 2009.
24. Chen, C. H., E. K. N. Yung, and B. J. Hu, "Miniaturised CPW-fed circularly polarized corrugated slot antenna with meander line loaded," *Electronics Letters*, Vol. 43, No. 25, Dec. 6, 2007.
25. Wong, K.-L., C.-C. Huang, and W.-S. Chen, "Printed ring slot antenna for circular polarization," *IEEE Transactions on Antennas and Propagation*, Vol. 50, No. 1, Jan. 2002
26. Chen, H. and H. T. Chen, "A CPW-fed dual-frequency monopole antenna," *IEEE Transactions on Antennas and Propagation*, Vol. 52, No. 4, Apr. 2004.
27. Sze, J. and K. Wong, "Bandwidth enhancement of a microstrip-line-fed printed wide-slot antenna," *IEEE Transactions on Antennas and Propagation*, Vol. 49, No. 7, Jul. 2001.
28. Chang, S. F. R., W. L. Chen, S. C. Chang, C. K. Tu, C. L. Wei, C. H. Chien, C. H. Tsai, J. Chen, and A. Chen, "A dual-band RF transceiver for multistandard WLAN applications," *IEEE Trans. Microw. Theory Tech.*, Vol. 53, 1048–1055, Mar. 2005.
29. Sze, J., C. I. G. Hsu, and S. C. Hsu, "Design of a compact dual-band annular-ring slot antenna," *IEEE Antennas and Wireless Propagation Letters*, Vol. 6, 2007.
30. Jou, C. F., J.-W. Wu, and C.-J. Wang, "Novel broadband monopole antennas with dual-band circular polarization," *IEEE Transactions on Antennas and Propagation*, Vol. 57, No. 4, Apr. 2009.